The underappreciated role of nonvolatile cations on aerosol ammonium-sulfate molar ratios

Hongyu Guo[1], Athanasios Nenes[1,2,3,4], Rodney J. Weber[1]

[1] School of Earth and Atmospheric Sciences, Georgia Institute of Technology, Atlanta, GA 30332, USA
[2] School of Chemical and Biomolecular Engineering, Georgia Institute of Technology, Atlanta, GA 30332, USA
[3] Institute for Chemical Engineering Sciences, Foundation for Research and Technology – Hellas, Patras, GR-26504, Greece
[4] Institute for Environmental Research and Sustainable Development, National Observatory of Athens, P. Penteli, Athens, GR-15236, Greece

Correspondence to: Rodney J. Weber, (rweber@eas.gatech.edu), Athanasios Nenes (athanasios.nenes@gatech.edu)

Abstract. Overprediction of fine particle ammonium-sulfate molar ratios (*R*) by thermodynamic models is suggested as evidence for an organic film that only inhibits the equilibration of gas phase ammonia (but not water or nitric acid) with aerosol sulfate and questions the equilibrium assumption long thought to apply for submicron aerosol. The ubiquity of such organic films implies significant impacts on aerosol chemistry. We test the organic film hypothesis by analyzing ambient observations with a thermodynamic model. Measurements show that the deviation between *R* from a molar ratio of 2 is correlated with sodium (Na^+), a nonvolatile cation (NVC), with no correlation to organic aerosol mass concentration or mass fraction. *R* predicted by the thermodynamic model is very sensitive to concentrations of Na^+ or NVC in general. Both *R* and ammonia gas-particle partitioning can accurately reproduce observations when small amounts of nonvolatile cations (NVC) are included in the thermodynamic analysis, whereas exclusion of NVCs results in predicted *R* consistently near 2. This happens because more NVCs shift pH higher, shifting NH_3-NH_4^+ equilibrium to favor the gas and resulting in less particle phase ammonium and lower *R*. When NVCs are present, but not included in the thermodynamic model, the missing cation is replaced with ammonium in the model (NH_3-NH_4^+ equilibrium shifts to the particle), resulting in higher *R*. Thus, poor representation of NVCs in the thermodynamic model leads to higher *R* than observed. None of these effects are associated with interactions between inorganic and organic aerosol components. These analyses are based on bulk aerosol composition measurements and assuming all species are internally mixed, however, similar results are found even if NVCs and sulfate and ammonium are largely externally mixed, as long as a small fraction of the sulfate is mixed with the NVCs. These results strongly challenge the postulated ability of organic films to perturb aerosol acidity and prevent ammonia from achieving gas-particle equilibrium for the conditions considered. Furthermore, the results demonstrate the limitations of using molar ratios to infer aerosol properties or processes that depend on particle pH.

1. Introduction

pH is a fundamental aerosol property that affects aerosol formation and composition through pH-sensitive reactions (Jang et al., 2002; Eddingsaas et al., 2010; Surratt et al., 2010) and gas-particle partitioning of semivolatile species (Guo et al., 2016; Guo et al., 2017a). Acidity also modulates aerosol toxicity and atmospheric nutrient supply to the oceans through changing transition metals solubility (Meskhidze et al., 2003; Nenes et al., 2011; Longo et al., 2016; Fang et al., 2017). Despite its importance, challenges in measuring fine mode particle pH have led to the use of measurable aerosol properties as acidity proxies, such as aerosol ammonium-sulfate ratio or ion balances (e.g. (Paulot and Jacob, 2014; Wang et al., 2016; Silvern et al., 2017)). Recent work has shown that acidity proxies are not uniquely related to pH because they do not capture the variability in particle water content, ion activity coefficients, or partial dissociation of species in the aerosol phase (Guo et al., 2015; Hennigan et al., 2015; Guo et al., 2016). A better method that constrains aerosol pH is comparison between a thermodynamic analysis and observations of gas-particle partitioning of semivolatile species that are sensitive to pH at the given environmental conditions (i.e., gas-particle concentration ratios near 1:1) (Guo et al., 2015; Hennigan et al., 2015; Guo et al., 2016; Weber et al., 2016; Guo et al., 2017a). NH_3-NH_4^+, HNO_3-NO_3^-, and HCl-Cl^- pairs often meet this condition. The method has been utilized for a range of meteorological conditions (RH, T) and gas/aerosol concentrations demonstrating that model predictions are often in agreement with observations.

It has been noted that thermodynamic models fail to accurately predict ammonium-sulfate molar ratios (Kim et al., 2015; Weber et al., 2016; Silvern et al., 2017). In the southeastern US, where total ammonium ($NH_x = NH_3 + NH_4^+$) is observed to be in large excess of particle sulfate, observed NH_4^+/SO_4^{2-} molar ratios are in the range of 1-2 (Hidy et al., 2014; Guo et al., 2015; Kim et al., 2015). Thermodynamic models predict very low pH (0.5 to 2) (Guo et al., 2015) and molar ratios close to 2 (Kim et al., 2015; Weber et al., 2016; Silvern et al., 2017). The molar ratio discrepancy has led to the hypothesis that thermodynamic predictions are incorrect because particles are coated by organic films that inhibit the condensation of NH_3 from the gas phase, which gives rise to the molar ratio discrepancy (Silvern et al., 2017). Such kinetic limitations, if prevalent, opposes the validity of aerosol thermodynamic equilibrium. This could significantly impact aerosol chemistry and acidity-mediated processes, given the large organic aerosol mass fractions worldwide (Zhang et al., 2007) and expected increasing organic mass fractions in the future due to changing emission, as seen with SO_2 emission reductions in the eastern US (Hand et al., 2012; Attwood et al., 2014; Hidy et al., 2014). The hypothesis of organic films, however, is in stark contrast to established literature showing that NH_3, water vapor, and HNO_3 equilibrate with organic-rich aerosols (Ansari and Pandis, 2000; Moya et al., 2001; Morino et al., 2006; Fountoukis et al., 2009; Guo et al., 2015; Guo et al., 2016; Guo et al., 2017a; Liu et al., 2017; Paulot et al., 2017). Such a film, as proposed by Silvern et al. (2017), selectively limits NH_3, but not H_2O and HNO_3 molecules that are both larger than NH_3 hence more difficult to diffuse through media. At low temperature or low relative humidity, particles may be in semi-liquid or glassy state and have very low diffusivity of molecules throughout its volume (Tong et al., 2011; Bones et al., 2012). This may severely limit gas-particle mass transfer of all components and require much longer time scales to equilibrate. However, such an effect has not been observed for the conditions in the eastern US, as there is good agreement between observed and predicted particle water, and partitioning of NH_3-NH_4^+ and HNO_3-NO_3^- when RH is sufficiently high (greater than 40%) that the aerosol is likely in a complete liquid state (Guo et al., 2015; Guo et al., 2016).

Other reasons that are unrelated to organic films may drive the molar ratio discrepancy. Most analyses of aerosol acidity, molar ratios and partitioning of semivolatile species do not consider variation of aerosol composition with size, which may translate to a large range of acidity and hence equilibrium composition (Keene et al., 1998; Nenes et al., 2011; Young et al., 2013;

Bougiatioti et al., 2016; Fang et al., 2017). The presence of soluble nonvolatile cations (NVCs, such as Na^+, K^+, Ca^{2+}, Mg^{2+}), which are often neglected in thermodynamic calculations because of their relatively minor contribution to aerosol mass and ion charge balance (e.g., (Kim et al., 2015; Silvern et al., 2017)), or because they are not routinely included in aerosol composition measurements (e.g., those made with an aerosol mass spectrometer), or are not well quantified due to high measurement limit of detections (LODs) relative to anion species, can affect acidity and molar ratios. Here we show, based on a bulk $PM_{2.5}$ aerosol analysis that ignoring even small amounts of NVC as inputs to the thermodynamic model results in predicted NH_4^+/SO_4^{2-} molar ratios close to 2, whereas including them brings model-predicted molar ratios into agreement with observed levels. We also assess the implications of a bulk analysis by comparing those conclusions to aerosol that is externally mixed.

2. Methods

Molar ratios definition: Two ammonium-sulfate aerosol molar ratios (mol mol^{-1}) are used in the following analysis,

$$R = \frac{\mathrm{NH_4^+}}{\mathrm{SO_4^{2-}}} \quad (1)$$

$$R_{\mathrm{SO_4}} = \frac{\mathrm{NH_4^+} - \mathrm{NO_3^-}}{\mathrm{SO_4^{2-}}} \quad (2)$$

Both are based on mole concentrations in units of μmol m^{-3}. R_{SO4} is a more narrowly defined molar ratio that excludes NH_4^+ associated with NO_3^-, because some fractions of ammonium sulfate and ammonium nitrate can be associated with different sized particles (Zhuang et al., 1999) and molar ratios are calculated based on bulk composition data ($PM_{2.5}$ or PM_1). This issue is discussed in more details below. The upper limit for R and R_{SO4} is 2 for a particle composition of pure $(NH_4)_2SO_4$, and a lower limit of 0 for R when SO_4^{2-} is associated with other cations instead of NH_4^+ (e.g. Na_2SO_4) or if there is free H_2SO_4 in the aerosol. A negative R_{SO4} can occur for conditions of high NO_3^- and low NH_4^+, SO_4^{2-} concentrations (e.g., $NaNO_3$), but are rare for ambient fine particles (at least not seen in the two data sets studied in this paper). R or R_{SO4} is typically observed in the range of 1 and 2 in the southeastern US (Hidy et al., 2014; Guo et al., 2015; Weber et al., 2016). In cases where NO_3^- levels are low relative to SO_4^{2-}, the two ratios, R_{SO4} and R, are equivalent, as is observed in the summertime southeastern US, where NO_3^- is typically ~0.2 μg m^{-3}, NH_4^+ ~1 μg m^{-3}, and SO_4^{2-} ~3 μg m^{-3} (Blanchard et al., 2013).

Data: Two datasets are used for analysis; the Southern Oxidant and Aerosol Study (SOAS) and the Wintertime Investigation of Transport, Emissions, and Reactivity (WINTER). The SOAS study was conducted from 1 June to 15 July in the summer of 2013 at a rural ground site in Centreville (CTR), AL, representative of the southeastern US background atmosphere in summer. $PM_{2.5}$ ions were determined with from Particle-Into-Liquid-Sampler coupled with an Ion Chromatograph (PILS-IC). The PILS-IC detects aerosol water-soluble anions and cations collected and diluted by deionized water to the extent of complete deprotonation of H_2SO_4 in the aqueous sample (Orsini et al., 2003). NH_3 was from chemical ionization mass spectrometer measurements (You et al., 2014). In the following, we only use $PM_{2.5}$ ion data from a 12-day period (11-23 June) of the SOAS campaign. This is only part of our SOAS data set, which involved measurement of $PM_{2.5}$ in the first half of the study and PM_1 in the second half. Periods of rainfall are not included in the analysis. The same data set was used to study pH sensitivity to sulfate and ammonia (Weber et al., 2016). $PM_{2.5}$ anion and cation data were also collected during SOAS, along with NH_3 and HNO_3 with a Monitor for AeRosols and GAses (MARGA) (Allen et al., 2015). These data support the PILS data analysis; the results are similar using either data set. The WINTER data was collected during 13 research aircraft flights from 1 February to 15 March 2015 mainly sampling over the northeastern US. We use PM_1 aerosol data collected with a High-Resolution Time-of-Flight Aerosol Mass

Spectrometer (hereafter referred to as AMS), which have been extensively compared to the PILS anion measurements also made in that study (Guo et al., 2016). Details of the these two campaigns and instruments, and calculations and verification of pH based on the observation datasets, have been described in Guo et al. (2015) and Guo et al. (2016), respectively.

In the following analysis, we focus on R for summertime data sets since NO_3^- was generally low, and R_{SO4} for wintertime data sets where higher NO_3^- concentrations were observed. Both datasets report highly acidic aerosols with average pH~1 (Guo et al., 2015; Guo et al., 2016). At these pH levels, aerosol sulfate can be in the partially deprotonated form of HSO_4^- instead of SO_4^{2-}. For example, 10% of the total sulfate is predicted to be HSO_4^- for the SOAS condition (see Fig. S1 in the supplement). Free form H_2SO_4, which requires even lower pH, is rare. The SO_4^{2-} in this study refers to the sum of total aqueous aerosol sulfate (SO_4^{2-}, HSO_4^-, and H_2SO_4), the same definition (i.e., S(VI)) used in Silvern et al. (2017), since aerosol instruments report total aqueous sulfate as just SO_4^{2-}. The same applies to NH_4^+ and NO_3^-. The AMS vaporizes aerosols and ionizes non-refractory species with a 70 eV electron impact ionization and also cannot distinguish the dissociation states of inorganic ions (DeCarlo et al., 2006).

Thermodynamic analysis of observations: We have used the thermodynamic model ISORROPIA-II (Fountoukis and Nenes, 2007) to determine the liquid water content and composition (including H^+) of an NH_4^+-SO_4^{2-}-NO_3^--Cl^--Na^+-Ca^{2+}-K^+-Mg^{2+}-water inorganic aerosol (or a subset therein) and its partitioning with corresponding gases in a number of different locations (Guo et al., 2015; Bougiatioti et al., 2016; Guo et al., 2016; Weber et al., 2016; Guo et al., 2017a; Guo et al., 2017b). As in all of these studies pH is defined as;

$$\mathrm{pH} = -\log_{10}\gamma_{H^+}H^+_{aq} = -\log_{10}\frac{1000\gamma_{H^+}H^+_{air}}{W_i + W_o} \cong -\log_{10}\frac{1000\gamma_{H^+}H^+_{air}}{W_i} \quad (3)$$

where γ_{H^+} is the hydronium ion activity coefficient (assumed = 1; note that the binary activity coefficients of ionic pairs, including H^+, is calculated in the model), H^+_{aq} (mol L^{-1}) the hydronium ion concentration in particle liquid water, and H^+_{air} (μg m^{-3}) the hydronium ion concentration per volume of air. W_i and W_o (μg m^{-3}) are particle water concentrations associated with inorganic and organic species, respectively. pH predicted solely with predicted W_i is fairly accurate. We found the pH was 0.15-0.23 units systematically lower than and highly correlated to (r^2 = 0.97) pH predicted with measured total particle water (W_i + W_o) in the southeast (which includes the SOAS study), where W_o accounted for 35% of total particle water (Guo et al., 2015). For simplicity, we therefore use W_i for the following pH calculations. ISORROPIA-II was run in "forward" mode to calculate gas-particle equilibrium concentrations based on the input of total concentration of various inorganic species (e.g., NH_3 + NH_4^+). In all cases we also chose a "metastable" (not "stable") solution, which assumes inorganic ions are associated with the aerosol components that are completely aqueous and contain no solid precipitates (H^+_{aq} is meaningless in a completely effloresced aerosol) and so restrict the analysis to conditions where RH > 40%.

Mixing State: Because the aerosol composition data is bulk PM_1 or $PM_{2.5}$, we also assumed that the particles were internally mixed and that pH did not vary with size. This assumes that bulk properties represent the aerosols, including pH, and that gas-particle partitioning was in thermodynamic equilibrium with one bulk mixture of inorganic ions. In the following, we perform the analysis of NVCs on molar ratios and pH under the totally internal mixture (bulk) assumption. Then in the discussion that follows, we consider how the results of this assumption affects our findings by assuming NVCs are largely externally mixed with sulfate. In the external mixing analysis, the bulk aerosol is split into two subgroups that can be viewed as species largely found in PM_1 (e.g., NH_4^+ and SO_4^{2-}) and species found in $PM_{1\text{-}2.5}$, which contains mostly the NVCs, NO_3^- and some SO_4^{2-} and NH_4^+. These two external mixtures are in equilibrium with the same gases, NH_3 and HNO_3, and so interact through these species (i.e.,

NH_4^+ and NO_3^- can move between the two subgroups). Nonvolatile species, such as SO_4^{2-} and NVCs (Na^+) remain in the original size class assumed at the start of the analysis. To determine the final composition of the two subgroups we iteratively solve for the equilibrium conditions for each subgroup, by sequentially performing the equilibrium for one subgroup than the other. The final solution is found when the composition of each group no longer changes and are in equilibrium with the same gas phase species (in this case, NH_3, HNO_3, and H_2O (water vapor)). Mass of each species (gas plus particle) is conserved at all times. The assumed starting fractions of the semivolatile species in the subgroups (i.e., NH_4^+ and NO_3^-) does not affect the final solution. Below we test how the extent of SO_4^{2-} mixing with the NVCs affects pH and *R* compared to the bulk analysis. Previous studies have shown that pH is size dependent and generally higher at larger size (Young et al., 2013; Bougiatioti et al., 2016; Fang et al., 2017). The pH of the two externally mixed group of particles differ, and may also differ from the bulk pH determined from the internally mixed case. For comparison to the bulk pH, the average pH of the external mixture can be determined by:

$$\mathrm{pH} = -\log_{10}\frac{1000\left(H^+_{air,subgroup\ 1}+H^+_{air,subgroup\ 2}\right)}{W_{i,subgroup\ 1}+W_{i,subgroup\ 2}} \quad (4)$$

ISORROPIA input data files for the analyses reported in this paper are available in the supplemental files.

3. Results

3.1 NVCs cause discrepancy in molar ratios (*R*) prediction

The SOAS data set: We first investigate the issue of *R* discrepancy using PILS-IC $PM_{2.5}$ data from a 12-day period of the SOAS campaign. To test the sensitivity of ISORROPIA-II predictions to NVCs, we ran the model with three different Na^+ concentration inputs, with all other inputs (referred as the base case) remaining the same. Inputs for the base case included: total ammonium ($NH_x = NH_4^+ + NH_3$), SO_4^{2-}, NO_3^-, and Cl^-. Ca^{2+}, Mg^{2+}, K^+ inputs were set to zero as they were mostly below detection limits. Three different Na^+ input concentrations were tested: (1) Measured $PM_{2.5}$ Na^+ from PILS-IC, including data below the LOD; (2) Na^+ determined from an ion charge balance, $Na^+ = 2SO_4^{2-} + NO_3^- + Cl^- - NH_4^+$ (unit: nmol m^{-3}), hereafter as inferred Na^+; (3) $Na^+ = 0$.

The LOD of PILS-IC Na^+ was 0.07 μg m^{-3}, close to the average Na^+ concentration (determined including values below detection limits) that was measured during this period. In the following, Na^+ data below the LOD is used in the analysis to increase the size of the data set. Data below LOD are identified in the figures throughout. Na^+ data below LOD generally agree with independent MARGA measurements of Na^+, see Fig. S2a in the supplement. As all other NVC, such as K^+, Ca^{2+} and Mg^{2+}, were also generally below the PILS-IC LOD and set to zero in the analysis, the charge balance predicted Na^+ should be viewed as the concentration of generic NVC concentrations with a valence of 1. Inferred Na^+ has a high uncertainty due to error propagation of NH_4^+, SO_4^{2-}, NO_3^-, and Cl^- measurements (see Fig. S2b). Inferred Na^+ is generally above zero indicating a cation deficiency, but 8 out of 229 points (3% of the data) were slightly below zero. In these cases, a small positive value of 0.005 μg m^{-3} was assigned to inferred Na^+. Including these data has no effect on the results because the observed *R* was ~2. The concentration of H^+ is ignored in the ion charge balance calculation since it is 2-3 orders of magnitude smaller than the major inorganic ions, even at these low pH (between 0 and 2). For example, the average $PM_{2.5}$ mole concentrations per volume of air for the ions measured by the PILS-IC were NH_4^+ = 35.4, SO_4^{2-} = 21.1, NO_3^- = 3.7, Na^+ = 2.9, and Cl^- = 0.82 nmol m^{-3}, compared to ISORROPIA-predicted H^+ = 0.31 nmol m^{-3}. Fig. 1a shows that the inferred Na^+ was always higher than measured Na^+. This is due to overestimation of Na^+ by assuming total aqueous aerosol sulfate as SO_4^{2-} and contributions from other NVCs (K^+, Mg^{2+}, and Ca^{2+}). The inferred Na^+ from PILS and MARGA generally agree with each other and also agree with the total NVCs from MARGA measurements before June 18. The larger differences after June 18 are likely from difficulties in detecting NVCs in low concentrations and accumulation of systematic errors in various ionic species measured by one or both of these instruments.

The SOAS study period investigated here includes an episode of high Na^+ associated with a sea-salt (NaCl) aerosol event (Fig. 1a). This provided an opportunity to assess the role of NVCs on pH when concentrations were substantially above LOD. Periods when Na^+ was closer to typical background levels and near or below the LOD lead to similar conclusions in the following analysis. The observed Na^+ is mainly associated with NO_3^- (Fig. 1a), and to a lesser degree with Cl^-. These ions are highly correlated (Na^+-NO_3^- $r^2 = 0.82$ and Na^+-Cl^- $r^2 = 0.64$) and indicate some level of "chloride depletion" as the observed Cl^-/Na^+ ratio was 0.24 ± 0.16 (mol mol^{-1}) (mean ± SD), whereas fresh sea salts would have a molar ratio close to 1 (Tang et al., 1997). Chloride depletion occurs when an acid, such as HNO_3, is mixed with NaCl producing HCl that evaporates since higher volatility than HNO_3 (Fountoukis and Nenes, 2007), resulting in a loss of Cl^- and H^+ (increase in pH). Cl^- concentrations were sufficiently small (0.03 ± 0.04 μg m^{-3}, LOD = 0.01 μg m^{-3}) compared to the dominant and nonvolatile anion SO_4^{2-} and HCl was not included in the model input, so Cl^- had negligible effect on ISORROPIA predictions of pH and molar ratios.

Fig. 1 shows the effect of Na^+ (i.e., NVCs in general) on ISORROPIA-predicted SO_4^{2-}, NH_4^+, NH_3, *R*, and pH. Fig. 1b and Fig. 1e show that measured and predicted sulfate (SO_4^{2-}) and total ammonium ($NH_x = NH_3 + NH_4^+$) are always identical. SO_4^{2-} is nonvolatile and so remains unchanged by the model (output = input). The model predicts the gas-particle partitioning by conserving NH_x, so the NH_x/SO_4^{2-} molar ratio is also always accurately predicted. Therefore, the discrepancy between modeled and measured *R* must result from variation in the model prediction of NH_x partitioning, i.e., the predicted NH_4^+ concentration. It is noteworthy that NH_x/SO_4^{2-} is practically always above 2, indicating excess NH_x compared to SO_4^{2-}. Under such conditions, it is sometimes interpreted that NH_3 must completely neutralize SO_4^{2-} (Kim et al., 2015; Silvern et al., 2017), but the thermodynamic model predicts $PM_{2.5}$ to be highly acidic, with a pH between 0 and 2 (Fig. 1h). This results from NH_4^+ being semivolatile and SO_4^{2-} being virtually nonvolatile at any atmospherically-relevant concentration and acidity (Weber et al., 2016).

Comparing measured to ISORROPIA-predicted NH_3-NH_4^+ partitioning (particle phase fraction of total ammonium, $\varepsilon(NH_4^+) = NH_4^+/NH_x$) can be used to test the model output to various Na^+ input concentrations. Fig. 1g and Fig. 2 shows very good agreement between measured and observed NH_3-NH_4^+ partitioning when measured Na^+ is used in the model. However, inferred Na^+ generally under-predicts $\varepsilon(NH_4^+)$, possibly because for this data set it over-predicts NVC levels, resulting in higher pH (Fig. 1h), and a higher pH shifts a fraction of the NH_4^+ to gas phase NH_3. Zero Na^+ shows the opposite (Fig. 1g and Fig. 2); $\varepsilon(NH_4^+)$ is over-predicted because predicted pH is too low for no NVCs in the model but actually present in the aerosol. A lower pH partitions more NH_3 to the particle phase ($\varepsilon(NH_4^+)$ is too high).

R also depends on the input Na^+ concentration. Fig. 1f shows the time series comparison between *R* for various Na^+ levels included in the ISORROPIA input. Fig. 3 shows the summary statistics for various comparisons of *R*. For the SOAS analyzed time period, for an ISORROPIA input of the base case and measured Na^+, the predicted *R* was on average 1.85 ± 0.17. Predicted *R* was significantly lower by inferred Na^+ at a mean of 1.43 ± 0.32, and the highest *R* at 1.97 ± 0.02 was found when zero Na^+ was used as model input (see Figs. 1f and 3). The average measured *R* was 1.70 ± 0.23 for all PILS data and 1.61 ± 0.19 excluding the points with Na^+ below LOD. The MARGA measurement of *R* is very similar. For example, MARGA measured *R* was 1.78 ± 0.18 for all data and 1.65 ± 0.15 for periods when PILS Na^+ was above LOD (Allen et al., 2015), see Fig. S3 in the supplement. (Fig. S4 shows a scatter plot of these comparisons for the three Na^+ cases). Overall, these results show: (1) when NVCs are most accurately measured (above LOD), ISORROPIA predicted *R* is in close agreement with measured *R* (t- test at $\alpha = 0.05$ confirms no statistical difference); (2) inferred Na^+ is overestimated for this data set and has higher uncertainty, resulting

in a lower predicted *R* than measured *R*; (3) when $Na^+ = 0$ is input, ISORROPIA always predicts $R \sim 2$, a consequence of electroneutrality of the aerosol aqueous phase.

Sensitivity of R and pH to NVCs: The sensitivities of *R* and pH to Na^+, or any other NVC, is of interest. The discrepancy in *R* has been shown to be resolved for this data set by adding small amounts of Na^+, either measured (when near or above LOD) or inferred from an ion charge balance analysis when not measured or significantly below the measurement method LOD. In the SOAS case, inferred Na^+ resulted in too low predicted *R* (Fig. 3), likely because of propagation of SO_4^{2-}, NH_4^+, and NO_3^- measurement errors, indicating that thermodynamic model prediction of *R* is sensitive to the model input concentrations of NVCs. Also, to assess a possible role of organic species in general (Pye et al., 2017) or organic films (Silvern et al., 2017) on *R* and pH, the sensitivity of *R* and pH to $PM_{2.5}$ NVC (i.e., Na^+) and organic aerosol (OA) mass fraction or total OA, is compared. Here we use Na^+ as an example since it was the highest NVC concentration measured in this study; K^+ and Mg^{2+} have similar effects. Ca^{2+} behaves differently due to $CaSO_4$ solids precipitating out of solution.

Fig. 4 shows that differences in measured *R* from a value of 2 (i.e., $\Delta R = R_{measured} - 2$) increases with measured Na^+, but does not depend on OA mass fraction (gray points) or OA concentration (see Fig. S5 in the supplement). These results are consistent with the bias in *R* being associated with poor representation (or lack of inclusion) of NVCs in the thermodynamic model, but inconsistent with expectations if OA had a significant effect on *R*. Fig. 4 also shows that ISORROPIA-predicted *R* also depends on Na^+. Predicted *R* with Na^+ in the model input minus predicted *R* without Na^+ decreases with increasing measured Na^+ and is highly correlated with Na^+ concentration (orthogonal linear regression, $\Delta R = (-1.74 \pm 0.03)\ Na^+ + (0.001 \pm 0.003)$, $r^2 = 0.93$). The decreasing trend in *R* with increasing Na^+ can be explained simply by the pH increasing with Na^+, as shown in Fig. 4c. With increasing pH, some NH_4^+ shifts to gas phase NH_3 (supplemental Fig. S8a), resulting in lower NH_4^+ and lower *R*.

From the regression slope, for the SOAS measurement period analyzed, an average measured Na^+ level of 0.06 μg m^{-3} causes a decrease in *R* of 0.10. At a Na^+ level of 0.3 μg m^{-3}, ΔR reaches decreases by 0.5, indicating a rapid decrease from $R = 2$ (no NVC) to $R = 1.5$ (with NVC) for these conditions (i.e., it depends on the base case). Thus, not only is ΔR highly correlated with Na^+, it is also highly sensitive to Na^+. This is not seen for the organic aerosol mass fraction, here used as a proxy for the thickness of a possible film as it constrains the organic volume per particle.

In comparison to *R*, pH is less sensitive to inclusion of Na^+, or other NVCs in general. ΔpH is only 0.07 for the average Na^+ level of 0.06 μg m^{-3}, and increases to 0.38 at 0.3 μg m^{-3} Na^+ (Fig. 4b). The magnitude of ΔpH is relatively small and consistent with our previous studies where we investigated the effects of sea-salt on pH (Guo et al., 2016; Weber et al., 2016). ΔpH would be higher in regions with more abundant NVC. For instance, a ΔpH of 0.8 unit was found in Pasadena, CA, where the average $PM_{2.5}$ Na^+ mass was 0.77 μg m^{-3} (Guo et al., 2017a). Differences in sensitivity of *R* and pH to Na^+ can also be seen based on linear regressions. The magnitude of the ΔR-Na^+ slope is 1.74 compared to ΔpH-Na^+ slope of 1.27 (Fig. 4). Sensitivities of pH and *R* (or R_{SO4}) to Na^+ are discussed further below, next we investigate NVC effects on *R* and pH for a very different data set.

The WINTER data set: The *R* discrepancy is investigated for a larger geographical scale, different region and different season by performing a similar analysis with the WINTER study data set collected from the NSF C-130 research aircraft during wintertime. In this case the aerosol inorganic composition data used in the analysis is from an AMS and is PM_1. In this study, NVCs were generally higher than those measured during SOAS, especially when the aircraft sampled near coastlines (e.g. PM_1

Na^+ = 0.23 μg m^{-3}). Also, PM_1 nitrate was comparable to sulfate, largely owing to lower temperatures (NO_3^- 13 nmol m^{-3} vs. SO_4^{2-} 11 nmol m^{-3}) (Guo et al., 2016). Therefore, R_{SO4} was calculated instead of R.

The base case input to ISORROPIA-II in this analysis included NH_4^+, SO_4^{2-}, and total nitrate (NO_3^- + HNO_3). (NH_3 should be included to determine NH_x for input, but was not measured. It was found to have a small effect on predicted pH; e.g., ~0.2 higher pH when including an NH_3 concentration of 0.10 μg m^{-3} determined from an iteration method (Guo et al., 2016)). Fig. 5a shows that ISORROPIA over-predicted R_{SO4} for the base case (i.e., when cations are not included) and that this deviation increases as molar ratios approach 2 when NVCs determined from an ion charge balance get smaller. (Note that the predicted R_{SO4} should be biased low since NH_4^+ was under-predicted due to lack of NH_3 data, resulting in some fraction of input particle phase NH_4^+ repartitioned in the model to the gas phase, thus the deviation is even worse than shown). Fig. 5a shows that R is highly sensitive to lack of inclusion of NVCs when their concentrations are very low. However, when concentrations of NVC reach zero, predicted and measured R_{SO4} converge to the expected value of 2 (dark blue symbols in Fig. 5a). At the other extreme, as predicted NVCs increase, predicted and measured R_{SO4} become closer and converge to a molar ratio of zero because NH_4^+ approaches zero (NVC have replaced NH_4^+). On average, predicted R_{SO4} was 1.68 ± 0.51 versus the measured value of 1.47 ± 0.43 and average predicted Na^+ concentration was 0.15 μg m^{-3} (which is comparable to the offline PILS fraction collector IC-measured PM_1 Na^+ of 0.23 μg m^{-3}).

In contrast to ISORROPIA-predicted R_{SO4} without NVCs, including NVCs brings predicted and measured ammonium-sulfate molar ratios into agreement throughout the range in charge balance (relating to inferred NVCs) (Fig. 5b). Again, NVC concentrations were determined as NVCs = $Na^+ = 2SO_4^{2-} + NO_3^- - NH_4^+$ (unit: nmol m^{-3}) where all NVC are assumed to be Na^+. (Results based on other NVCs are shown in supplemental Fig. S6. K^+ and Mg^{2+} work similarly to Na^+, while Ca^{2+} can precipitate sulfate in the form of $CaSO_4$ and so cannot be used). Overall, Na^+ is chosen as a proxy NVC in our dataset because in this case it constitutes most of the NVC mass and does not precipitate out of solution. The choice of Na^+ as a NVC proxy, although appropriate here, is not generally applicable, such as in regions with considerable dust contributions, treating NVC as "equivalent Na^+" in the thermodynamic calculations can result in large prediction errors (e.g., (Fountoukis et al., 2009)). The linear regression result is $R_{SO4,predicted}$ = (1.05 ± 0.01) $R_{SO4,measured}$ + (−0.12 ± 0.01), r^2 = 0.99. As found for the SOAS data set, again, the molar ratio bias from the thermodynamic model is simply a matter of not including small amounts of NVC (e.g., in this case on average 0.15 μg m^{-3} Na^+ or 0.26 μg m^{-3} K^+). The average amount of inferred Na^+ from the ion charge balance in this case is smaller than what was measured offline during the study; PM_1 Na^+ of 0.23 μg m^{-3} (Guo et al., 2016). The analysis using measured PM_1 Na^+ results in highly scattered data due to the high sensitivities of R_{SO4} to NVC and the significant Na^+ measurement uncertainty at these low levels given the analytical method used in this study.

3.2 Implications of not including NVC on predicting gas-particle partitioning and historical trends in molar ratios

Sensitivity of semi-volatile species partitioning to NVCs: In our datasets, inferred Na^+ (or K^+, Mg^{2+}) from an ion charge balance that groups all NVCs into one species is an upper limit of the NVCs because it assumes complete dissociation of all dissolved ionic species. Additional errors can occur if other ions are also missing, but this approach satisfies electroneutrality. Comparing ISORROPIA predictions that includes the other major species, but with an inferred Na^+ input versus Na^+ = 0 input results in an average difference in pH by 0.32 for SOAS and 0.49 for WINTER, respectively. Even though the effect of NVC on pH may appear relatively small, the impact on predicted partitioning of a semivolatile species can be significant due to the highly non-

linear response of NH_3-NH_4^+ or HNO_3-NO_3^- partitioning to pH (i.e., S curve) (Guo et al., 2016; Guo et al., 2017a). For example, as shown in supplemental Fig. S7, a 0.3 unit pH bias in SOAS campaign could cause ~ 20% bias in $\varepsilon(NH_4^+)$ or $\varepsilon(NO_3^-)$ prediction when $\varepsilon(NH_4^+)$ or $\varepsilon(NO_3^-)$ = 50%, or no bias at all when the species are completely in one phase, $\varepsilon(NH_4^+)$ or $\varepsilon(NO_3^-)$ = 0% or 100%. For the WINTER study, a 0.5 pH bias causes up to 30% bias in $\varepsilon(NH_4^+)$ or $\varepsilon(NO_3^-)$. These partitioning biases may constitute a significant source of bias for aerosol nitrate formation, especially if the total nitrate present in the gas-aerosol system is significant. In fact, the bias from the NVC may completely change the predicted response of nitrate to aerosol emissions and lead to errors in the predicted vs. observed trends in pH, such as was seen in the southeastern US (Vasilakos et al., 2017).

Effect of NVCs in trends in pH and R in the southeastern US: One curious observation that the organic film hypothesis (Silvern et al, 2017) attempted to address was the decreasing trend in *R* in the southeastern US despite the substantial drop in sulfate. Weber et al., (2016) noted this and proposed that it could be explained by NH_4^+ volatility. However, the thermodynamic model predictions of R_{SO4} in that study did not find a comparable decreasing R_{SO4} rate with time (see Fig. 6a), since the SOAS study mean PILS-IC Na^+ concentration of 0.03 μg m^{-3} was applied to all historical data. With a constant ISORROPIA Na^+ input of 0.03 μg m^{-3}, predicted R_{SO4} was nearly constant at ~2 for the input $SO_4^{2=}$ range (Fig. 6a) and would only rapidly decrease below 1 μg m^{-3} SO_4^{2-} (See Fig. 2b in the paper). Repeating the calculations using Na^+ inferred from the ion charge balance of Na^+-NH_4^+-SO_4^{2-}-NO_3^-, determined for each daily data point in the historical data set, results in good agreement between observed and ISORROPIA-predicted R_{SO4} (Fig. 6 & Fig. S8). It also results in ISORROPIA-predicted decreasing R_{SO4} rate of –0.017 yr^{-1}, fairly close to the measured rate at the SOAS site (Centerville, AL) of -0.021 yr^{-1} (see Fig. 6a), and in the range of the R_{SO4} trend of –0.01 to –0.03 yr^{-1} reported by Hidy et al. (2014) for SEARCH sites throughout the southeast. In contrast, using these different Na^+ input concentrations did not change the trends in ISORROPIA-predicted pH; in both cases it remained relatively constant (Fig. 6b), but as expected the pH was slightly higher with higher input Na^+ concentrations. Thus, including daily estimates of NVC in ISORROPIA, the conclusion that $PM_{2.5}$ pH has remained largely constant over the last 15 years remains, but the unexpected decreasing R_{SO4} trend appears to be accounted for. These observations can all be explained by volatility of NH_4^+, as discussed in Weber et al. (2016), without need to invoke organic effects on the ammonia partitioning.

4. Discussion

Internal vs External Mixtures: This analysis has been based on the assumption that all ions were internally mixed (e.g., bulk $PM_{2.5}$ or PM_1). Although over time, gas-particle and particle-particle interactions will lead to complete internally mixed systems, aerosol near their source regions tend to be externally mixed. Typical ambient conditions can be expected to exist somewhere between these two extreme cases. We address this here by studying how the conclusions described above are affected by the degree of mixing of NVCs with ammonium and sulfate – as the other species, being semi-volatile, quickly equilibrate.

$PM_{2.5}$ sea salts (or other NVCs) are often not well mixed with ammonium and sulfate because of their different sources. NVCs are largely produced by mechanical means and so mainly in the coarse mode, with a tail extending into the fine mode (Whitby, 1978). In contrast, ammonium and sulfate are mostly formed through gas-phase processes and mostly reside in the accumulation mode (e.g., (Whitby, 1978; Zhuang et al., 1999; Fang et al., 2017)). For the SOAS PILS-IC data set, NH_4^+ and SO_4^{2-} were highly correlated (r^2 = 0.88), but NH_4^+ and Na^+ (r^2 = 0.07) or SO_4^{2-} and Na^+ (r^2 = 0.17) were not. In contrast, $PM_{2.5}$ Na^+ and NO_3^- (r^2 = 0.82) or Na^+ and Cl^- (r^2 = 0.64) were highly correlated, consistent with internal mixing of most Na^+, NO_3^-, and Cl^- ions, leading to depletion of some Cl^- through evaporation of HCl. Rapid scavenging of HNO_3 by sea salt aerosols is well established (Hanisch

and Crowley, 2001; Meskhidze et al., 2005), with equilibrating time scales 3-10 hours for HNO_3 uptake by 1-3 μm sea spray aerosols (Meng and Seinfeld, 1996; Fridlind and Jacobson, 2000).

NVCs can also be associated small amounts of sulfate. For example, sea salt aerosols are largely composed of NaCl but also include sulfate found in sea water, approximately 8% (g g^{-1}) of all ions (~25% SO_4^{2-}/Na^+ mass ratio) (sea water salinity of 35 psu) (DOE, 1994). In addition, sulfur enrichment and chloride depletion in aged sea salt aerosols are possible by uptake of H_2SO_4 or oxidation of dissolved SO_2 by O_3 (McInnes et al., 1994; O'Dowd et al., 1997). These secondary produced sulfates are normally referred as non-sea-salt sulfates, to be distinguished from sea-salt sulfate that is naturally in sea waters (Tang et al., 1997). Many studies have reported sulfate-containing sea salt aerosols with some degrees of internal mixing (Andreae et al., 1986; McInnes et al., 1994; Murphy et al., 1998; Laskin et al., 2002). In summary, a realistic external mixing state of the SOAS fine particles is that most of NH_4^+ and SO_4^{2-} are in PM_1 and Na^+ with associated anions (NO_3^- and Cl^-) and at least small amounts of NH_4^+ and SO_4^{2-} in $PM_{1\text{-}2.5}$ (particles with sizes 1-2.5 μm). This is illustrated in Fig. 7a. Particle size distributions measured in the southeast US also support these types of particle mixing state (Fang et al., 2017).

Explanation for role of NVCs on R based on bulk (internal mixture) analysis: Assuming the ions are all internally mixed, the observations relating *R* to NVCs, and deviations in *R* between models and observations can be readily explained. First, when NVC such as Na^+ are present in the ambient aerosol and not included in the thermodynamic model and some fraction of the associated anion pair is, the thermodynamic model will predict higher NH_4^+ than observed because the model will partition greater levels of available semivolatile cations (i.e., NH_3) to the particle phase (NH_4^+) to conserve NH_x and make up for the missing NVCs. This leads to a predicted *R* near 2. The trends in measured *R* with measured Na^+ are also expected. As noted before, measured *R* becomes increasingly less than 2 as measured Na^+ increase because at higher Na^+ bulk aerosol pH increases (Fig. 3c), resulting in lower $\varepsilon(NH_4^+)$ (see NH_4^+ S curve in supplemental Fig. S7), shifting NH_4^+ to gas phase NH_3. Other NVCs have similar effects as Na^+, as long as soluble forms of the salts are observed (e.g., $NaNO_3$, Na_2SO_4, KNO_3, K_2SO_4, $Ca(NO_3)_2$, $Mg(NO_3)_2$). We have shown with this bulk analysis that accurately including NVCs in the thermodynamic analysis appears to largely resolves the disparity in predicted and measured *R*. But the bulk analysis is only an approximation of the actual aerosol mixing state. Can assuming an internal mixture roughly represent the behavior of externally mixed aerosols in terms of the effect of NVCs on *R*, pH, and partitioning of semivolatile species? To assess this, we consider the behavior of external mixing cases.

Explanation for the role of NVCs on R based on external mixture analysis: An extreme (and unrealistic) external mixture is where PM_1 is composed of all the measured NH_4^+, SO_4^{2-} and $PM_{1\text{-}2.5}$ is composed of all the measured Na^+ (all NVCs), NO_3^-, and Cl^-. NH_3, HNO_3, HCl, and H_2O (water vapor) can still equilibrate between these externally mixed particle types (see Fig. 7a), given the relatively short equilibrating time scales for these sizes of particles (Dassios and Pandis, 1999; Cruz et al., 2000; Fountoukis et al., 2009). As Fig. 7b shows, for the extreme external mixing case (i.e. 0% sulfate in $PM_{1\text{-}2.5}$), predicted *R*, combined from PM_1 and $PM_{1\text{-}2.5}$, is close to 2, deviating from the lower predicted *R* of 1.66 ± 0.13 from the internal mixture. This is due to the vastly different pH of PM_1 (0.6) and $PM_{1\text{-}2.5}$ (4.1) (Fig. 7c), so, all NH_4^+ is predicted to be in PM_1, and all NO_3^- is predicted to be in $PM_{1\text{-}2.5}$.

For more realistic mixing cases where some fraction of the sulfate is mixed with NVCs, the combined *R* of the external mixture decreases rapidly as more SO_4^{2-} is mixed with Na^+ in $PM_{1\text{-}2.5}$. Higher Na^+ concentrations generally require more SO_4^{2-} to obtain agreement in *R* between external and internal mixtures (scatter plots are shown as supplemental Fig. S9). At 20% SO_4^{2-} fraction

in $PM_{1\text{-}2.5}$, the average levels of predicted *R* start to converge between external and internal mixtures (Fig. 7b). The difference in pH between PM_1 and $PM_{1\text{-}2.5}$ is also reduced to within one pH unit (Fig. 7c). With these small differences in pH, NH_4^+ can condense both externally-mixed aerosol groups. For example, PM_1 and $PM_{1\text{-}2.5}$ NH_4^+ are predicted to be 0.67 μg m^{-3} and 0.04 μg m^{-3}, respectively (equal to the sum of the measured $PM_{2.5}$ NH_4^+ of 0.71 μg m^{-3}). For the external mixed cases, not including Na^+ in the model input causes an *R* overprediction the same way as we have explained for the internal mixture. From this analysis, which is based only on data when Na^+ was above the LOD, predicted *R* for the bulk and external mixture are the same when on average 18 ± 7% of the $PM_{2.5}$ SO_4^{2-} is in the $PM_{1\text{-}2.5}$ size range (i.e., mixed with Na^+). This is comparable to inferences of mixing based on size-resolved aerosol measurements in the southeast (e.g., Fang et al. (2017) shows ~30% $PM_{2.5}$ SO_4^{2-} mass in $PM_{1\text{-}2.5}$). Less internal mixing of SO_4^{2-} with Na^+ is needed when Na^+ concentrations are lower. For example, for Na^+ at the LOD of 0.07 μg m^{-3} (for the PILS-IC operated during SOAS), only 5% of the SO_4^{2-} mixed with Na^+ produces the same results as the bulk totally internal mixture analyses (see supplemental Fig. S10).

The difference between the internally and externally mixed system is not as great as may be expected, especially for particle pH and liquid water (W_i) (Fig. 7c and Fig. 7d). Since liquid water levels are determined as the sum of the water associated with the various salts, the bulk liquid water generally equals the sum of the two externally mixed liquid water concentrations, based on the Zdanovskii–Stokes–Robinson (ZSR) relationship (Zdanovskii, 1936; Stokes and Robinson, 1966). The PM_1 liquid water dominates over $PM_{1\text{-}2.5}$, making the combined pH of the external mixture nearly identical to PM_1 pH (see Equation 4 for combined pH calculation). The combined pH of the external mixture is also similar to that of internal mixture, regardless of the SO_4^{2-} fractions.

5. Summary

Including NVCs in the thermodynamic model largely resolves the ammonium-sulfate molar ratio ($R = NH_4^+/SO_4^{2-}$) discrepancy, based on our data set, which is representative of the southeastern US. Since only small amounts of NVC can significantly affect *R*, measurement limitations (high NVC LODs or not measured at all) can lead to substantial differences in observed and thermodynamic model predicted *R*. We show that this bias in *R* (ISORROPIA-predicted *R* with Na^+ minus ISORROPIA-predicted *R* without Na^+) is correlated with and highly sensitive to measured Na^+, but not correlated with organic aerosol mass or mass fraction. Furthermore, the difference in measured *R* from a ratio of 2 (2 minus observed *R*) is correlated to measured Na^+ (NVCs) and not correlated with organic aerosol mass or mass fraction. If organic films were limiting mass transfer, the discrepancy in *R* should worsen as the films become thicker. We find the opposite. These results provide strong evidence for the role of NVCs but not bulk organic aerosol species or organic films in the molar ratio discrepancy.

Excluding minor amounts of fine mode NVC in thermodynamic calculations results in predicted *R* near 2, which is generally higher than observed values. This results from the model criteria for aerosol electrical neutrality and semivolatile NH_4^+ has to be increased to compensate the missing NVCs. Less absolute discrepancy is associated with predicted particle pH with or without NVC because pH is on a logarithmic scale of H_{aq}^+ and the range of pH is larger than that of *R* (or R_{SO4}) in the eastern US. For example, the observed ranges in molar ratios (*R* or R_{SO4} from 0 to 2) are less than those of pH (from -1 to 3) in the two data sets investigated in this study (Guo et al., 2015; Guo et al., 2016). However, neglecting NVC can induce pH biases that could result in significant partitioning errors for semivolatile species like ammonium, nitrate, chloride, and even organic acids, under certain conditions. Because NVCs are often minor constituents of fine particles, especially for submicron particles, implying low

ambient concentrations and high measurement uncertainties, assessing thermodynamic model predictions through molar ratios is problematic. If NVCs were not measured or significantly below the measurement LOD, an ion charge balance could be used to inferred an upper limit on NVC concentrations, but addition of measurement uncertainties can lead to uncertain results.

A motivation for the organic effects on ammonia partitioning (Silvern et al., 2017) was the observed R_{SO4} decreasing trend over the past 15 years in the southeastern US. Fully considering NVCs doesn't change the finding of nearly constant fine particle pH in the southeast (summertime) despite the large sulfate reductions in the past 15 years, but it does now produce agreement with the observed R_{SO4} decreasing trend. Finally, although the analysis was performed assuming total internal mixtures of aerosol components, since only bulk $PM_{2.5}$ composition data were available, we show that external mixtures of NVCs and sulfate produce similar results, with the only requirement that small amounts of sulfate are mixed with the NVC-rich particles. As a final note, because molar ratios are sensitive to NVCs, and NVC concentrations are often very low and can be highly uncertain, use of molar ratios to test the thermodynamic model should be done with caution. Molar ratios are also poor pH proxies and not recommended to evaluate aerosol acidity (Guo et al., 2015; Hennigan et al., 2015; Guo et al., 2016).

Acknowledgements. This work was supported by the National Science Foundation (NSF) under grant AGS-1360730. The WINTER data is provided by NCAR/EOL under sponsorship of the National Science Foundation (http://data.eol.ucar.edu/). AN acknowledges support from an EPA STAR grant and the European Research Council Consolidator Grant 726165 - PyroTRACH.

References

Allen, H. M., Draper, D. C., Ayres, B. R., Ault, A., Bondy, A., Takahama, S., Modini, R. L., Baumann, K., Edgerton, E., Knote, C., Laskin, A., Wang, B., and Fry, J. L.: Influence of crustal dust and sea spray supermicron particle concentrations and acidity on inorganic NO_3^- aerosol during the 2013 Southern Oxidant and Aerosol Study, Atmospheric Chemistry and Physics, 15, 10669-10685, doi: 10.5194/acp-15-10669-2015, 2015.

Andreae, M. O., Charlson, R. J., Bruynseels, F., Storms, H., R, V. A. N. G., and Maenhaut, W.: Internal mixture of sea salt, silicates, and excess sulfate in marine aerosols, Science, 232, 1620-1623, doi: 10.1126/science.232.4758.1620, 1986.

Ansari, A. S., and Pandis, S. N.: The effect of metastable equilibrium states on the partitioning of nitrate between the gas and aerosol phases, Atmospheric Environment, 34, 157-168, doi: 10.1016/s1352-2310(99)00242-3, 2000.

Attwood, A. R., Washenfelder, R. A., Brock, C. A., Hu, W., Baumann, K., Campuzano-Jost, P., Day, D. A., Edgerton, E. S., Murphy, D. M., Palm, B. B., McComiskey, A., Wagner, N. L., de Sa, S. S., Ortega, A., Martin, S. T., Jimenez, J. L., and Brown, S. S.: Trends in sulfate and organic aerosol mass in the Southeast U.S.: Impact on aerosol optical depth and radiative forcing, Geophysical Research Letters, 41, 7701-7709, doi: 10.1002/2014gl061669, 2014.

Blanchard, C. L., Hidy, G. M., Tanenbaum, S., Edgerton, E. S., and Hartsell, B. E.: The Southeastern Aerosol Research and Characterization (SEARCH) study: Spatial variations and chemical climatology, 1999–2010, Journal of the Air & Waste Management Association, 63, 260-275, doi: 10.1080/10962247.2012.749816, 2013.

Bones, D. L., Reid, J. P., Lienhard, D. M., and Krieger, U. K.: Comparing the mechanism of water condensation and evaporation in glassy aerosol, Proceedings of the National Academy of Sciences of the United States of America, 109, 11613-11618, doi: 10.1073/pnas.1200691109, 2012.

Bougiatioti, A., Nikolaou, P., Stavroulas, I., Kouvarakis, G., Weber, R., Nenes, A., Kanakidou, M., and Mihalopoulos, N.: Particle water and pH in the Eastern Mediterranean: Sources variability and implications for nutrients availability, Atmospheric Chemistry and Physics, 16, 4579-4591, doi: 10.5194/acp-16-4579-2016, 2016.

Cruz, C. N., Dassios, K. G., and Pandis, S. N.: The effect of dioctyl phthalate films on the ammonium nitrate aerosol evaporation rate, Atmospheric Environment, 34, 3897-3905, doi: 10.1016/S1352-2310(00)00173-4, 2000.

Dassios, K. G., and Pandis, S. N.: The mass accommodation coefficient of ammonium nitrate aerosol, Atmospheric Environment, 33, 2993-3003, doi: 10.1016/S1352-2310(99)00079-5, 1999.

DeCarlo, P. F., Kimmel, J. R., Trimborn, A., Northway, M. J., Jayne, J. T., Aiken, A. C., Gonin, M., Fuhrer, K., Horvath, T., Docherty, K. S., Worsnop, D. R., and Jimenez, J. L.: Field-deployable, high-resolution, time-of-flight aerosol mass spectrometer, Analytical chemistry, 78, 8281-8289, doi: 10.1021/ac061249n, 2006.

DOE: Handbook of Methods for the Analysis of the Various Parameters of the Carbon Dioxide System in Sea Water. Version 2, edited by: Dickson, A. G., and Goyet, C., ORNL/CDIAC-74, 1994.

Eddingsaas, N. C., VanderVelde, D. G., and Wennberg, P. O.: Kinetics and Products of the Acid-Catalyzed Ring-Opening of Atmospherically Relevant Butyl Epoxy Alcohols, Journal of Physical Chemistry A, 114, 8106-8113, doi: 10.1021/Jp103907c, 2010.

Fang, T., Guo, H., Zeng, L., Verma, V., Nenes, A., and Weber, R. J.: Highly Acidic Ambient Particles, Soluble Metals, and Oxidative Potential: A Link between Sulfate and Aerosol Toxicity, Environmental science & technology, 51, 2611-2620, doi: 10.1021/acs.est.6b06151, 2017.

Fountoukis, C., and Nenes, A.: ISORROPIA II: a computationally efficient thermodynamic equilibrium model for K^+-Ca^{2+}-Mg^{2+}-NH_4^+-Na^+-SO_4^{2-}-NO_3^--Cl^--H_2O aerosols, Atmospheric Chemistry and Physics, 7, 4639-4659, doi: 10.5194/acp-7-4639-2007, 2007.

Fountoukis, C., Nenes, A., Sullivan, A., Weber, R., Van Reken, T., Fischer, M., Matias, E., Moya, M., Farmer, D., and Cohen, R. C.: Thermodynamic characterization of Mexico City aerosol during MILAGRO 2006, Atmospheric Chemistry and Physics, 9, 2141-2156, doi: 10.5194/acp-9-2141-2009, 2009.

Fridlind, A. M., and Jacobson, M. Z.: A study of gas-aerosol equilibrium and aerosol pH in the remote marine boundary layer during the First Aerosol Characterization Experiment (ACE 1), Journal of Geophysical Research: Atmospheres, 105, 17325-17340, doi: 10.1029/2000jd900209, 2000.

Guo, H., Xu, L., Bougiatioti, A., Cerully, K. M., Capps, S. L., Hite, J. R., Carlton, A. G., Lee, S. H., Bergin, M. H., Ng, N. L., Nenes, A., and Weber, R. J.: Fine-particle water and pH in the southeastern United States, Atmospheric Chemistry and Physics, 15, 5211-5228, doi: 10.5194/acp-15-5211-2015, 2015.

Guo, H., Sullivan, A. P., Campuzano-Jost, P., Schroder, J. C., Lopez-Hilfiker, F. D., Dibb, J. E., Jimenez, J. L., Thornton, J. A., Brown, S. S., Nenes, A., and Weber, R. J.: Fine particle pH and the partitioning of nitric acid during winter in the northeastern United States, Journal of Geophysical Research: Atmospheres, 121, 10355-10376, doi: 10.1002/2016jd025311, 2016.

Guo, H., Liu, J., Froyd, K. D., Roberts, J. M., Veres, P. R., Hayes, P. L., Jimenez, J. L., Nenes, A., and Weber, R. J.: Fine particle pH and gas–particle phase partitioning of inorganic species in Pasadena, California, during the 2010 CalNex campaign, Atmospheric Chemistry and Physics, 17, 5703-5719, doi: 10.5194/acp-17-5703-2017, 2017a.

Guo, H., Weber, R. J., and Nenes, A.: High levels of ammonia do not raise fine particle pH sufficiently to yield nitrogen oxide-dominated sulfate production, Scientific Reports, 7, doi: 10.1038/s41598-017-11704-0, 2017b.

Hand, J. L., Schichtel, B. A., Malm, W. C., and Pitchford, M. L.: Particulate sulfate ion concentration and SO_2 emission trends in the United States from the early 1990s through 2010, Atmospheric Chemistry and Physics, 12, 10353-10365, doi: 10.5194/acp-12-10353-2012, 2012.

Hanisch, F., and Crowley, J. N.: The heterogeneous reactivity of gaseous nitric acid on authentic mineral dust samples, and on individual mineral and clay mineral components, Physical Chemistry Chemical Physics, 3, 2474-2482, doi: 10.1039/b101700o, 2001.

Hennigan, C. J., Izumi, J., Sullivan, A. P., Weber, R. J., and Nenes, A.: A critical evaluation of proxy methods used to estimate the acidity of atmospheric particles, Atmospheric Chemistry and Physics, 15, 2775-2790, doi: 10.5194/acp-15-2775-2015, 2015.

Hidy, G. M., Blanchard, C. L., Baumann, K., Edgerton, E., Tanenbaum, S., Shaw, S., Knipping, E., Tombach, I., Jansen, J., and Walters, J.: Chemical climatology of the southeastern United States, 1999-2013, Atmospheric Chemistry and Physics, 14, 11893-11914, doi: 10.5194/acp-14-11893-2014, 2014.

Jang, M., Czoschke, N. M., Lee, S., and Kamens, R. M.: Heterogeneous atmospheric aerosol production by acid-catalyzed particle-phase reactions, Science, 298, 814-817, doi: 10.1126/science.1075798, 2002.

Keene, W. C., Sander, R., Pszenny, A. A. P., Vogt, R., Crutzen, P. J., and Galloway, J. N.: Aerosol pH in the marine boundary layer: A review and model evaluation, Journal of Aerosol Science, 29, 339-356, doi: 10.1016/s0021-8502(97)10011-8, 1998.

Kim, P. S., Jacob, D. J., Fisher, J. A., Travis, K., Yu, K., Zhu, L., Yantosca, R. M., Sulprizio, M. P., Jimenez, J. L., Campuzano-Jost, P., Froyd, K. D., Liao, J., Hair, J. W., Fenn, M. A., Butler, C. F., Wagner, N. L., Gordon, T. D., Welti, A., Wennberg, P. O., Crounse, J. D., St Clair, J. M., Teng, A. P., Millet, D. B., Schwarz, J. P., Markovic, M. Z., and Perring, A. E.: Sources, seasonality, and trends of southeast US aerosol: an integrated analysis of surface, aircraft, and satellite observations with the GEOS-Chem chemical transport model, Atmospheric Chemistry and Physics, 15, 10411-10433, doi: 10.5194/acp-15-10411-2015, 2015.

Laskin, A., Iedema, M. J., and Cowin, J. P.: Quantitative Time-Resolved Monitoring of Nitrate Formation in Sea Salt Particles Using a CCSEM/EDX Single Particle Analysis, Environmental Science & Technology, 36, 4948-4955, doi: 10.1021/es020551k, 2002.

Liu, M., Song, Y., Zhou, T., Xu, Z., Yan, C., Zheng, M., Wu, Z., Hu, M., Wu, Y., and Zhu, T.: Fine particle pH during severe haze episodes in northern China, Geophysical Research Letters, 44, 5213-5221, doi: 10.1002/2017gl073210, 2017.

Longo, A. F., Feng, Y., Lai, B., Landing, W. M., Shelley, R. U., Nenes, A., Mihalopoulos, N., Violaki, K., and Ingall, E. D.: Influence of Atmospheric Processes on the Solubility and Composition of Iron in Saharan Dust, Environ Sci Technol, 50, 6912-6920, doi: 10.1021/acs.est.6b02605, 2016.

McInnes, L. M., Covert, D. S., Quinn, P. K., and Germani, M. S.: Measurements of chloride depletion and sulfur enrichment in individual sea-salt particles collected from the remote marine boundary layer, Journal of Geophysical Research, 99, doi: 10.1029/93jd03453, 1994.

Meng, Z., and Seinfeld, J. H.: Time scales to achieve atmospheric gas-aerosol equilibrium for volatile species, Atmospheric Environment, 30, 2889-2900, doi: 10.1016/1352-2310(95)00493-9, 1996.

Meskhidze, N., Chameides, W. L., Nenes, A., and Chen, G.: Iron mobilization in mineral dust: Can anthropogenic SO_2 emissions affect ocean productivity?, Geophysical Research Letters, 30, 2085, doi: 10.1029/2003gl018035, 2003.

Meskhidze, N., Chameides, W. L., and Nenes, A.: Dust and pollution: A recipe for enhanced ocean fertilization?, Journal of Geophysical Research, 110, D03301, doi: 10.1029/2004jd005082, 2005.

Morino, Y., Kondo, Y., Takegawa, N., Miyazaki, Y., Kita, K., Komazaki, Y., Fukuda, M., Miyakawa, T., Moteki, N., and Worsnop, D. R.: Partitioning of HNO_3 and particulate nitrate over Tokyo: Effect of vertical mixing, Journal of Geophysical Research, 111, doi: 10.1029/2005jd006887, 2006.

Moya, M., Ansari, A. S., and Pandis, S. N.: Partitioning of nitrate and ammonium between the gas and particulate phases during the 1997 IMADA-AVER study in Mexico City, Atmospheric Environment, 35, 1791-1804, doi: 10.1016/s1352-2310(00)00292-2, 2001.

Murphy, D. M., Anderson, J. R., Quinn, P. K., McInnes, L. M., Brechtel, F. J., Kreidenweis, S. M., Middlebrook, A. M., Posfai, M., Thomson, D. S., and Buseck, P. R.: Influence of sea-salt on aerosol radiative properties in the Southern Ocean marine boundary layer, Nature, 392, 62-65, doi: Doi 10.1038/32138, 1998.

Nenes, A., Krom, M. D., Mihalopoulos, N., Van Cappellen, P., Shi, Z., Bougiatioti, A., Zarmpas, P., and Herut, B.: Atmospheric acidification of mineral aerosols: a source of bioavailable phosphorus for the oceans, Atmospheric Chemistry and Physics, 11, 6265-6272, doi: 10.5194/acp-11-6265-2011, 2011.

O'Dowd, C. D., Smith, M. H., Consterdine, I. E., and Lowe, J. A.: Marine aerosol, sea-salt, and the marine sulphur cycle: a short review, Atmospheric Environment, 31, 73-80, doi: 10.1016/s1352-2310(96)00106-9, 1997.

Orsini, D. A., Ma, Y., Sullivan, A., Sierau, B., Baumann, K., and Weber, R. J.: Refinements to the particle-into-liquid sampler (PILS) for ground and airborne measurements of water soluble aerosol composition, Atmospheric Environment, 37, 1243-1259, doi: 10.1016/s1352-2310(02)01015-4, 2003.

Paulot, F., and Jacob, D. J.: Hidden cost of U.S. agricultural exports: particulate matter from ammonia emissions, Environ Sci Technol, 48, 903-908, doi: 10.1021/es4034793, 2014.

Paulot, F., Paynter, D., Ginoux, P., Naik, V., Whitburn, S., Van Damme, M., Clarisse, L., Coheur, P. F., and Horowitz, L. W.: Gas-aerosol partitioning of ammonia in biomass burning plumes: Implications for the interpretation of spaceborne

observations of ammonia and the radiative forcing of ammonium nitrate, Geophysical Research Letters, doi: 10.1002/2017gl074215, 2017.

Pye, H. O. T., Zuend, A., Fry, J. L., Isaacman-VanWertz, G., Capps, S. L., Appel, K. W., Foroutan, H., Xu, L., Ng, N. L., and Goldstein, A. H.: Coupling of organic and inorganic aerosol systems and the effect on gas-particle partitioning in the southeastern United States, Atmospheric Chemistry and Physics Discussions, 1-25, doi: 10.5194/acp-2017-623, 2017.

Silvern, R. F., Jacob, D. J., Kim, P. S., Marais, E. A., Turner, J. R., Campuzano-Jost, P., and Jimenez, J. L.: Inconsistency of ammonium–sulfate aerosol ratios with thermodynamic models in the eastern US: a possible role of organic aerosol, Atmospheric Chemistry and Physics, 17, 5107-5118, doi: 10.5194/acp-17-5107-2017, 2017.

Stokes, R. H., and Robinson, R. A.: Interactions in Aqueous Nonelectrolyte Solutions .I. Solute-Solvent Equilibria, Journal of Physical Chemistry, 70, 2126-2130, doi: 10.1021/J100879a010, 1966.

Surratt, J. D., Chan, A. W., Eddingsaas, N. C., Chan, M., Loza, C. L., Kwan, A. J., Hersey, S. P., Flagan, R. C., Wennberg, P. O., and Seinfeld, J. H.: Reactive intermediates revealed in secondary organic aerosol formation from isoprene, Proceedings of the National Academy of Sciences of the United States of America, 107, 6640-6645, doi: 10.1073/pnas.0911114107, 2010.

Tang, I. N., Tridico, A. C., and Fung, K. H.: Thermodynamic and optical properties of sea salt aerosols, Journal of Geophysical Research: Atmospheres, 102, 23269-23275, doi: 10.1029/97jd01806, 1997.

Tong, H. J., Reid, J. P., Bones, D. L., Luo, B. P., and Krieger, U. K.: Measurements of the timescales for the mass transfer of water in glassy aerosol at low relative humidity and ambient temperature, Atmospheric Chemistry and Physics, 11, 4739-4754, doi: 10.5194/acp-11-4739-2011, 2011.

Vasilakos, P., Russell, A. G., Weber, R. J., and Nenes, A.: Understanding nitrate formation in a world with less sulfate, In review, 2017.

Wang, G., Zhang, R., Gomez, M. E., Yang, L., Levy Zamora, M., Hu, M., Lin, Y., Peng, J., Guo, S., Meng, J., Li, J., Cheng, C., Hu, T., Ren, Y., Wang, Y., Gao, J., Cao, J., An, Z., Zhou, W., Li, G., Wang, J., Tian, P., Marrero-Ortiz, W., Secrest, J., Du, Z., Zheng, J., Shang, D., Zeng, L., Shao, M., Wang, W., Huang, Y., Wang, Y., Zhu, Y., Li, Y., Hu, J., Pan, B., Cai, L., Cheng, Y., Ji, Y., Zhang, F., Rosenfeld, D., Liss, P. S., Duce, R. A., Kolb, C. E., and Molina, M. J.: Persistent sulfate formation from London Fog to Chinese haze, Proceedings of the National Academy of Sciences of the United States of America, 113, 13630-13635, doi: 10.1073/pnas.1616540113, 2016.

Weber, R. J., Guo, H., Russell, A. G., and Nenes, A.: High aerosol acidity despite declining atmospheric sulfate concentrations over the past 15 years, Nature Geoscience, 9, 282-285, doi: 10.1038/ngeo2665, 2016.

Whitby, K. T.: The physical characteristics of sulfur aerosols, Atmospheric Environment (1967), 12, 135-159, doi: 10.1016/0004-6981(78)90196-8, 1978.

You, Y., Kanawade, V. P., de Gouw, J. A., Guenther, A. B., Madronich, S., Sierra-Hernandez, M. R., Lawler, M., Smith, J. N., Takahama, S., Ruggeri, G., Koss, A., Olson, K., Baumann, K., Weber, R. J., Nenes, A., Guo, H., Edgerton, E. S., Porcelli, L., Brune, W. H., Goldstein, A. H., and Lee, S. H.: Atmospheric amines and ammonia measured with a chemical ionization mass spectrometer (CIMS), Atmospheric Chemistry and Physics, 14, 12181-12194, doi: 10.5194/acp-14-12181-2014, 2014.

Young, A. H., Keene, W. C., Pszenny, A. A. P., Sander, R., Thornton, J. A., Riedel, T. P., and Maben, J. R.: Phase partitioning of soluble trace gases with size-resolved aerosols in near-surface continental air over northern Colorado, USA, during winter, Journal of Geophysical Research: Atmospheres, 118, 9414-9427, doi: 10.1002/jgrd.50655, 2013.

Zdanovskii, A. B.: Trudy Solyanoi Laboratorii Akad, Nauk SSSR, 2, 1936.

Zhang, Q., Jimenez, J. L., Canagaratna, M. R., Allan, J. D., Coe, H., Ulbrich, I., Alfarra, M. R., Takami, A., Middlebrook, A. M., Sun, Y. L., Dzepina, K., Dunlea, E., Docherty, K., DeCarlo, P. F., Salcedo, D., Onasch, T., Jayne, J. T., Miyoshi, T., Shimono, A., Hatakeyama, S., Takegawa, N., Kondo, Y., Schneider, J., Drewnick, F., Borrmann, S., Weimer, S., Demerjian, K., Williams, P., Bower, K., Bahreini, R., Cottrell, L., Griffin, R. J., Rautiainen, J., Sun, J. Y., Zhang, Y. M., and Worsnop, D. R.: Ubiquity and dominance of oxygenated species in organic aerosols in anthropogenically-influenced Northern Hemisphere midlatitudes, Geophysical Research Letters, 34, L13801, doi: 10.1029/2007gl029979, 2007.

Zhuang, H., Chan, C. K., Fang, M., and Wexler, A. S.: Size distributions of particulate sulfate, nitrate, and ammonium at a coastal site in Hong Kong, Atmospheric Environment, 33, 843-853, doi: 10.1016/S1352-2310(98)00305-7, 1999.

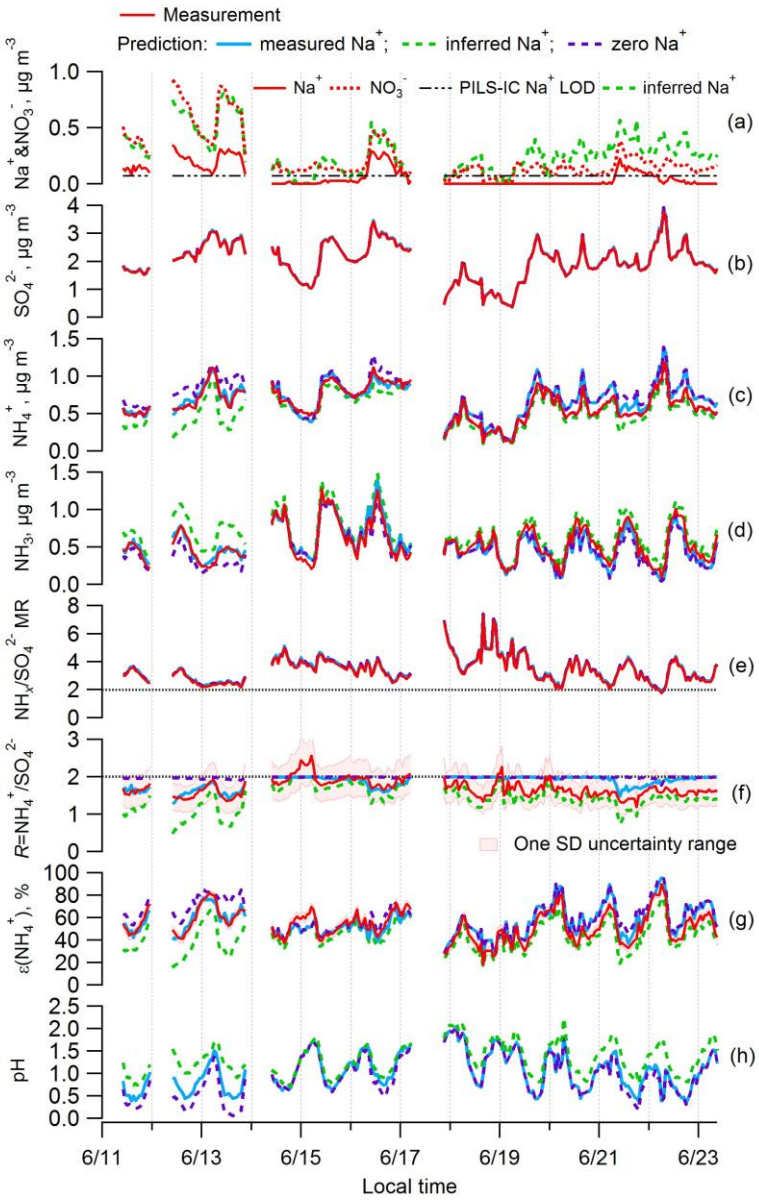

Figure 1. Time series of various measured and ISORROPIA-predicted parameters and $PM_{2.5}$ component concentrations for the SOAS study. Specific plots are as follows: (a) Na^+ and NO_3^-, (b) SO_4^{2-}, (c) NH_4^+, (d) NH_3, (e) total ammonium ($NH_x = NH_4^+ + NH_3$) to sulfate molar ratio (NH_x/SO_4^{2-}), (f) ammonium-sulfate ratio ($R = NH_4^+/SO_4^{2-}$), (g) particle-phase fractions of total ammonium, $\varepsilon(NH_4^+)$, and (h) particle pH. ISORROPIA-predicted results for the base case and three different Na^+ inputs are shown: measured Na^+ in blue, Na^+ from an ion charge balance ($Na^+ = 2SO_4^{2-} + NO_3^- + Cl^- - NH_4^+$, μmol m^{-3}) in green representing generic nonvolatile cation (NVC) concentrations, and zero Na^+ in purple.

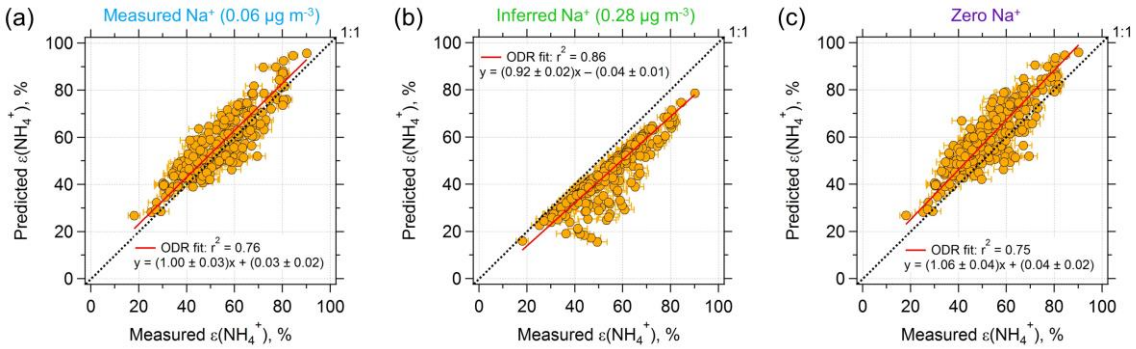

Figure 2. Comparisons of predicted and measured particle phase fractions of total ammonium, $\varepsilon(NH_4^+) = NH_4^+/NH_x$. (a) The model prediction is based on an ISORROPIA input of measured Na^+, NH_x, SO_4^{2-}, NO_3^-, Cl^-. (b) Same model input, but Na^+ is inferred from an ion charge balance and (c) Na^+ is set to zero. Orthogonal distance regression (ODR) fits are shown and uncertainties in the fits are one standard deviation (SD). Uncertainty of measured $\varepsilon(NH_4^+)$ is derived from error propagation of NH_4^+ (20%) and NH_3 (6.8%) measurements. Best agreement is achieved by using measured Na^+ as input.

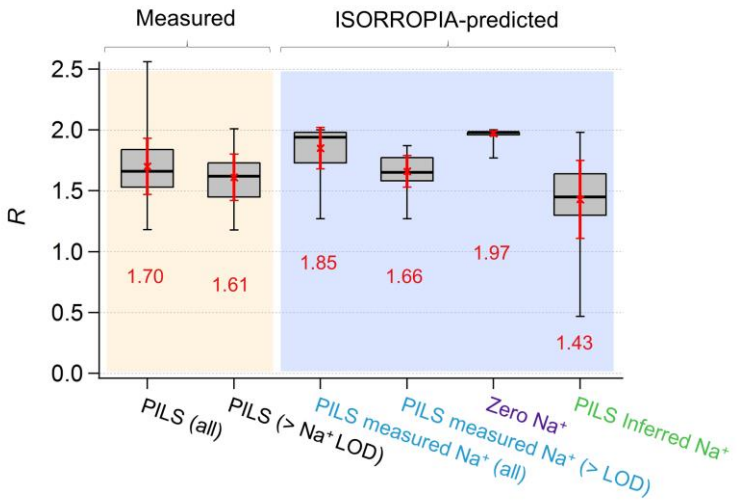

Figure 3. Comparisons of $PM_{2.5}$ ammonium-sulfate molar ratios (*R*) between measurements and ISORROPIA-predictions for the base case but with differing Na^+ inputs. Data are from the SOAS study. Red numbers are the means and red error bars are one SD. Standard box-whisker plots are shown, with 100% and 0% data indicated by black error bars. Top and bottom of box are the interquartile ranges (75% and 25%) centered around the median value (50%). Comparisons include all data and periods when measured Na^+ > LOD of 0.07 µg/m^3. Inferred Na^+ is calculated from an ion charge balance with no other NVC included.

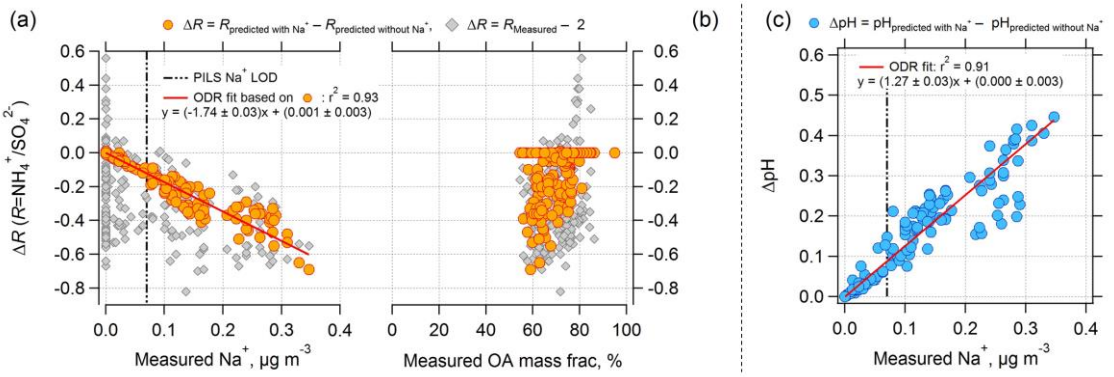

Figure 4. Effect of nonvolatile cations (NVC) on the $PM_{2.5}$ ammonium-sulfate molar ratios (*R*) and pH as a function of measured Na^+ concentration and organic aerosol (OA) mass fractions for the SOAS data set studied. Plot (a) is Δ*R* versus measured Na^+, (b) Δ*R* versus measured OA mass fraction (OA mass divided total particle mass reported from AMS), and (c) ΔpH versus measured Na^+. Grey diamonds in plots (a) and (b) are for Δ*R* equal to the measured *R* minus 2. Orange circular points are for Δ*R* equal to ISORROPIA-predicted *R* with measured Na^+ included in the model input minus ISORROPIA-predicted *R* without Na^+ in the model input. ΔpH in plot (c) is determined in a similar way. Δ*R* is negative since including Na^+ in the thermodynamic model results in *R* lower than 2, whereas not including Na^+ results in an *R* close to 2 (see Fig. 3). ODR fits are shown and uncertainties in the fits are one standard deviation. A plot similar to (b), but versus OA mass concentration can be found as Fig. S5. The vertical dotted line is the Na^+ LOD of 0.07 µg/m^3.

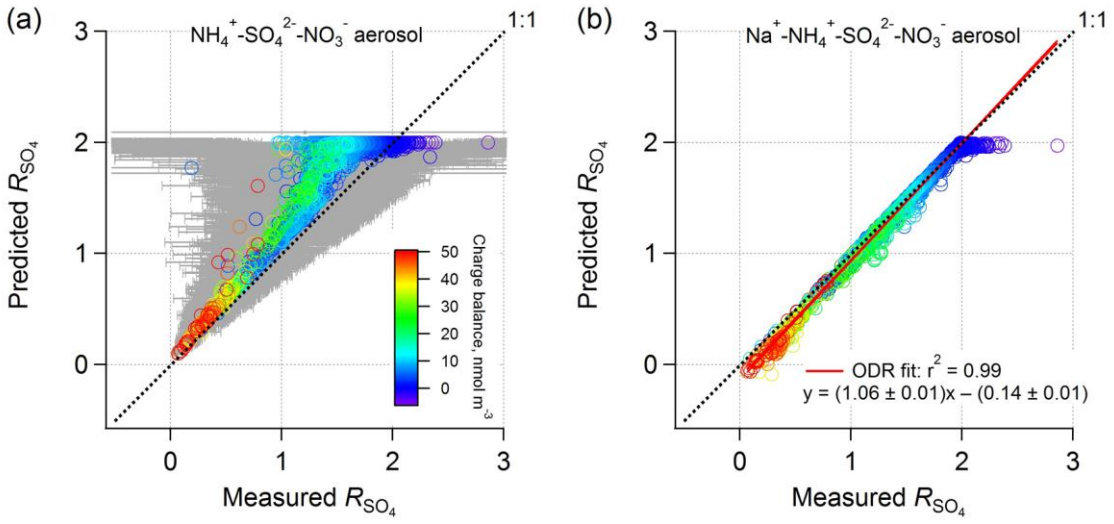

Figure 5. Comparison between PM_1 ISORROPIA-predicted R_{SO4} and AMS-measured R_{SO4} (R_{SO4} = ($NH_4^+ - NO_3^-$)/SO_4^{2-}) (mol mol^{-1}), where the ISORROPIA-prediction is based on (a) NH_4^+, SO_4^{2-}, NO_3^- aerosol and (b) Na^+, NH_4^+, SO_4^{2-}, NO_3^- aerosol, and both include HNO_3 to calculate total nitrate for the model input. All measurement data are from the WINTER study. NVCs were determined by an ion charge balance with the predicted molar concentration shown by symbol color. Error bars were determined by propagated uncertainties for R_{SO4} based on a 35% AMS measurement uncertainty for NH_4^+, SO_4^{2-}, and NO_3^- (Bahreini et al., 2009). Error bars are larger at higher ratios due to subtraction of higher concentrations of nitrate and so subject to greater measurement error. Data points with low SO_4^{2-} levels (<0.2 μg m^{-3}; 9% of the total points) were excluded due to high uncertainties.

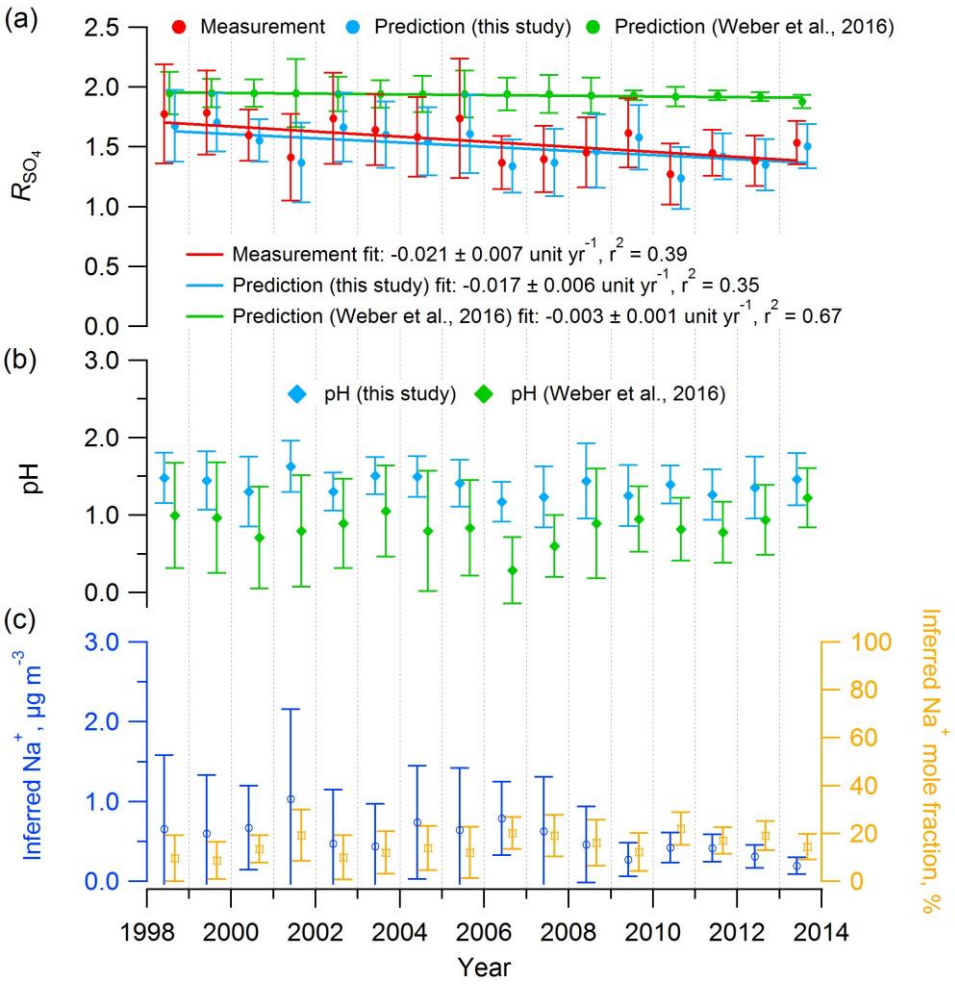

Figure 6. Mean summer (June–August) trends in (a) measured and predicted R_{SO4}, (b) predicted $PM_{2.5}$ pH, and (c) inferred Na^+ concentration and mole fraction at the SEARCH-CTR site. Na^+ was inferred from an ion charge balance of Na^+-NH_4^+-SO_4^{2-}-NO_3^-. ISORROPIA inputs include the measured $PM_{2.5}$ composition (NH_4^+, SO_4^{2-}, NO_3^-) and meteorological data (RH, T) at CTR. In all cases, R_{SO4} and pH were estimated with ISORROPIA-II run in forward mode with an assumed NH_3 level of 0.36 µg m^{-3}, the mean concentration from the SOAS study (CTR site, summer 2013), due to limited NH_3 data before 2008. Historical NH_3 mean summer concentrations at CTR were 0.2 µg m^{-3} (2004-2007) (Blanchard et al., 2013) and 0.23 ± 0.14 µg m^{-3} (2008-2013) (Weber et al., 2016). Error bars represent daily data ranges (SD). Linear regression fits are shown and uncertainties in the fits are one SD. 41 data points out of 609 (7%) with observed daily mean R_{SO4} above 3 were considered outliers and not shown (if included the fit slope is −0.023 ± 0.008 unit yr^{-1}).

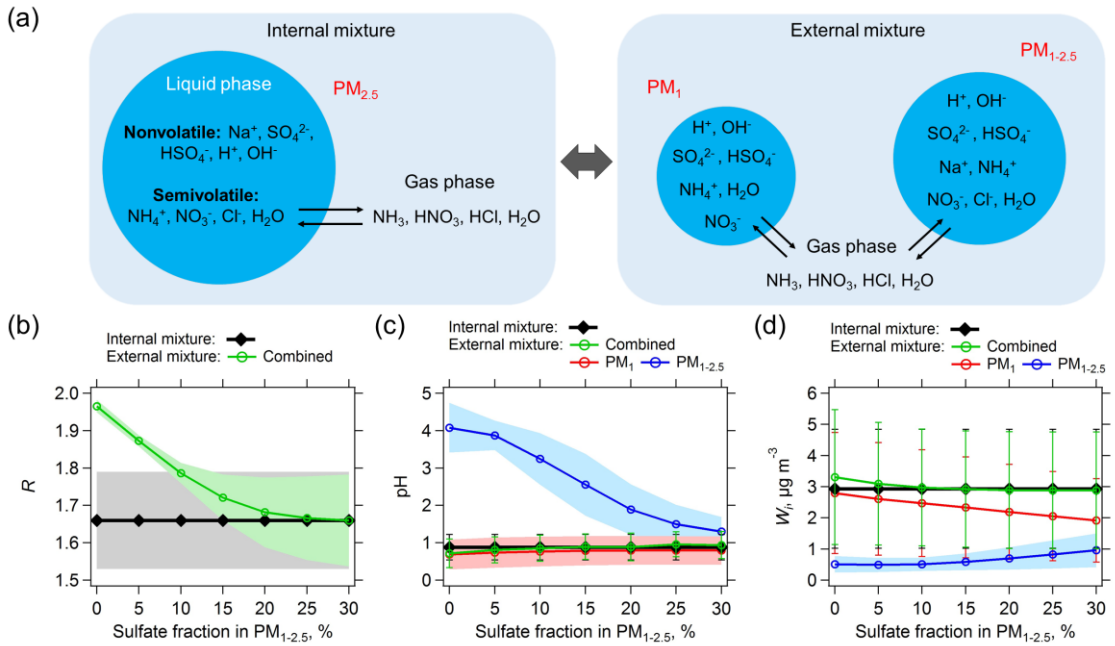

Figure 7. (a) Schematic of assumed internally and externally mixed aerosols. NVCs (here represented by Na^+) are all assumed in $PM_{1\text{-}2.5}$ for the external mixing case. The two externally mixed aerosol groups (PM_1 and $PM_{1\text{-}2.5}$) are in equilibrium with the same gases. The internal mixed case has bulk $PM_{2.5}$ composition (PM_1 + $PM_{1\text{-}2.5}$) together with gases as model input. The predicted molar ratio (*R*), pH, and liquid water ($\boldsymbol{W_i}$) of the internally and externally mixed aerosols are summarized in (b), (c), and (d), respectively. The x-axis is the sulfate fraction assumed in $PM_{1\text{-}2.5}$, with the remaining sulfate in PM_1. For the analysis shown here only data for which measured Na^+ was above the LOD are utilized. Lower Na^+ concentrations require smaller fractions of SO_4^{2-} in the $PM_{1\text{-}2.5}$ range for agreement with the bulk analysis (e.g., 5% for PILS-IC Na^+ LOD of 0.07 µg m^{-3}). Standard deviations of the data are shown as error bars or shaded zones.